



## Improving the performance of water-based drilling fluid using amino acid-modified graphene oxide nanocomposite as a promising additive

M.A. Betiha, M.M. Dardir, H. Abuseda, N.A. Negm\*, H.E. Ahmed



CrossMark

*Egyptian Petroleum Research Institute, Nasr City, Cairo, Egypt.*

### Abstract

It is possible to take advantage of nanomaterials' properties to improve water-based drilling fluids' flux and physical properties. In this paper, glycine methyl ester hydrochloride was synthesized, and the chemical structure was verified to be used as a surface modifier of graphene oxide. At the same time, graphene oxide was prepared from graphite and chlorinated with thionyl chloride, and a nucleophilic substitution reaction was performed to increase the hydrophilicity of graphene oxide. FTIR, Raman, HRTEM, and XRD techniques have identified the prepared and obtained materials from chlorinated graphene oxide's reaction with glycine methyl ester hydrochloride. The glycine-modified graphene oxide (GO) was evaluated as drilling-fluid additives at different concentrations (2.66%, 5.32%, and 10.64%) to enhancement the thermal stability of water-based drilling fluid and reducing the filtration loss. The obtained results confirmed that the successful glycine-modified graphene oxide/bentonite to enhance both thermal stability (up to 350 °F) and filtration loss.

**Key words:** Graphene; nanomaterial; water-based drilling fluids; filter loss; rheology.

### 1. Introduction

Hydrocarbons represent the main source of energy globally, and therefore it has become a challenge to reach deep oil tanks with high temperatures and pressures and the ability to drill them economically. Drilling fluids always have a pivotal role in achieving successful drilling operations, especially concerning the challenges associated with formation damage (Betiha, Mohamed A. et al., 2020; Faroughi et al., 2018). Therefore, in particular, water-based drilling fluids are constantly developing to introduce new additives that give them distinct properties that meet the requirements of the standards required to deal with bore problems. Bentonite is the highest percentage in drilling fluids, and its role is to transfer the drilling cuttings from the well to the well's surface. It has another very important characteristic: to reduce the mud cake permeability and reduce the loss of fluids added to the water-based drilling paste. The key to obtaining unique properties of drilling fluids depends on how much the bentonite clay layers are dispersed in the water, and therefore, many types of research are concerned with preserving the bentonite clay layers in a state of dispersion (Luo et al., 2018; Zhong et al., 2015). The principal rule of

stabilizing is interacting with the minerals' surface and consequently neutralized, and aggregation is obstructed. Among the stabilizers that increase the efficiency of bentonite clay polymers (sodium 4-styrene sulfonate) and lignin-derived polymers, the heavy metals bound to the polymer and low thermal stability cause some environmental problems (Kelessidis et al., 2007). Drilling fluid mud (montmorillonite) suffers from chemical instability at two temperatures of more than 250 °C, resulting in its inability to retain fluids and increases fluid loss in the formation, thus reducing its effectiveness well as the difficulty to use at high pressures and temperatures (Kelessidis et al., 2006).

With the increasing interest in nanotechnology, there are a large number of studies concerned with the possibility of using nanoparticles associated with or added to polymers in the petroleum industry, especially in the field of their use as additives to drilling fluids to improve rheological and filtration properties (Li et al., 2016; Ponmani et al., 2016; Rafati et al., 2018). A study has been made to add different iron oxide concentrations to the water drilling fluid by Vryzas et al. (Vryzas et al., 2015), and the authors found that adding 0.5 wt% of iron

\*Corresponding author e-mail: [nabelnegm@hotmail.com](mailto:nabelnegm@hotmail.com); (Nabil Negm).

Receive Date: 04 December 2020, Revise Date: 22 December 2020, Accept Date: 23 December 2020

DOI: 10.21608/EJCHEM.2020.52219.3075

©2021 National Information and Documentation Center (NIDOC)

oxide nanoparticles leads to a reduction in the fluid loss by 42.5%.

Graphene is a two-dimensional honeycomb carbon layered material with distinct properties such as large surface area, excellent electrical conductivity, and good mechanical strength. Graphene can be formulated in many different ways, one of which is using a chemical reaction. Oxidation of graphite with strong chemical oxidants can provide graphene oxide in nanoscale sheets with proven efficiency as additives to drilling fluids and have shown almost better ability to control fluid loss than polymers (Kosynkin et al., 2012; Saleh et al., 2020).

Xuan et al. (Xuan et al., 2014) compared the effect of graphene oxide, polyanionic-cellulose, and sulfomethyl-phenol-formaldehyde resin as additives to control the fluid loss at temperatures below 180 °C of water-based mud. They found that graphene oxide proved superior to these additives at relatively low concentrations. Dmitry et al. (Kosynkin et al., 2012) demonstrated that adding graphene oxide to water-based drilling fluids improved fluid loss. The authors also stated that the addition of graphene oxide with different nanoscale sizes improved the drilling fluid's performance, as it achieved a 6 mL (fluid loss) over 30 minutes compared to the industrial polymer (7.2 mL).

This paper evaluates the potential of modified graphene oxide with substance 1 (in different concentrations) as an additive to drilling fluids to enhance its thermal stability to reduce the amount of filtration loss. The chemical and physical properties of the modified graphene oxide compound and the drilling fluids samples were also evaluated with X-ray diffraction (XRD), Raman spectroscopy, and transmission electron microscopy (HRTEM). In addition, drilling fluid samples were mixed according to standard API requirements to obtain the rheological features, including plastic viscosity (PV), apparent viscosity (AP), Gel strength (GL), and yield point (YP), and filter loss at different conditions of temperature. To make a comparison between the additives influences on the rheological properties, the following mixtures were used; water/bentonite mixture, water/ bentonite/modified graphene oxide

## 2. Materials and technique.

### 2.1 Materials

Bentonite clay was provided from Sphinx Company. Natural flake graphite, potassium permanganate (KMnO<sub>4</sub>, 97%), sulfuric acid (H<sub>2</sub>SO<sub>4</sub>, 95.0-98.0%), hydrochloric acid (HCl, 37%), thionyl chloride (SOCl<sub>2</sub> 97%), methanol (anhydrous, 99.8%), hydrogen peroxide solution (H<sub>2</sub>O<sub>2</sub>, 30%), glycine (NH<sub>2</sub>CH<sub>2</sub>COOH, ≥98.5%) and sodium nitrate (NaNO<sub>3</sub>, ≥99.0%) were purchased from Merck.

### 2.2. Preparation of graphene oxide (GO)

The chemical conversion of graphite powder to graphene oxide was carried out following a modified Hammers approach with a slight modification procedure (Hassan et al., 2020; Marcano et al., 2010). A mixture of concentrated sulfuric acid and phosphoric acid is prepared in a ratio of 9: 1, and an amount of this mixture of 27 mL is added to 0.29 g of graphene powder under stirring. After the graphite is dispersed in the mixture, the mixture is cooled down to 0 °C. Then, KMnO<sub>4</sub> (1.35) adds up to the mixture with great care while monitoring the rise in temperature (high temperature should be avoided, especially when the mixture's viscosity increased for safety). After completing the addition, the mixture is left under stirring for 3 h, after which the mixture is poured into a container containing crushed ice containing hydrogen peroxide (1.5 mL). The temperature was raised very slowly until the mixture's color turned golden yellow, then 30 ml of hydrochloric acid (10%) was added to the mixture. Graphene oxide is separated by centrifugation and washed several times with distilled water until a pH of 6.7 is reached. Graphite oxide was soaked in dichloroethane for 24 hours, filtered, and dried at 80 °C.

### 2.2. Preparation of modified graphene oxide (glycine-GO)

Glycine-modified graphene oxide was prepared by the Pytlakowska method (Pytlakowska et al., 2016) with some modification. First, glycine methyl ester hydrochloride was prepared due to the lack of solubility of glycine in organic solvents as follows: glycine (10 g) was added portion by portion to 100 mL of thionyl chloride, and methanol mixture (1:20) under stirring and flow of nitrogen gas at 0 °C and then the temperature was allowed to rise automatically to the room temperature for a period of 12 hours, then at 50 °C for another 12 h. After removing the excess solvents, the resulting material was precipitated in diethyl ether and separated by filtration. The second step includes preparing chlorinated graphene oxide as follows; graphene oxide (1 g) was added to 160 mL of thionyl chloride diluted with 5 mL of THF. After experimenting at 50 °C for 24 hours under nitrogen flow, thionyl chloride was removed under vacuum at 70 °C. The resulting solid was treated with 10 g of glycine methyl ester hydrochloride in THF (100 mL) at a temperature of 70 °C under nitrogen flow.

The product was separated from the excess glycine methyl ester hydrochloride by centrifugation. The material was washed continuously by re-dispersing the glycine-GO material in water using ultrasonic and re-separating by centrifugation.

### 2.3. Characterization

FTIR spectra were carried out on a PerkinElmer-FTIR, the USA, in the range of 400  $\text{cm}^{-1}$  to 4000  $\text{cm}^{-1}$ . Raman spectroscopy data was obtained from Lab. RAM-HR Evolution Horiba Co. instruments using a 532 nm excitation light source. X-ray diffraction patterns were recorded by D8-Discovery–Bruker Co. at 40 kV and 40 Am (1600W) at speed scan 0.01. High-resolution transmission electron microscopy (Jeol-200, Japan) was used to monitor the layered graphene oxide's morphology. Viscometer (Fann 35 viscometer) is used to obtain rheological parameters

### 2.3.1. Preparation of drilling mud samples

According to the API method, the original drilling fluids sample was prepared, whereby 6% of bentonite clay was swelled in half a liter of water. The sample was rolled in a cylindrical furnace for 16 h prior to testing to simulate the conditions under which the drilling mud would be used. The bentonite sample was then poured into the aging cells and pressed to an appropriate back pressure to prevent the clay sample fluids from evaporating. This step is followed by adding modified graphene oxide in different proportions to the mixture of drilling fluids (the original drilling fluid, bentonite in water), and the previous processes are repeated to simulate the API method to determine the role of graphene in improving thermal stability and reducing filtration loss. In addition, the tests were carried out at three temperatures (100 °F, 200 °F, 300 °F, 350 °F).

### 2.3.2. Rheological properties of drilling fluids and calculations

Rheological parameters include determination of apparent viscosity (AP), plastic viscosity PV, yield point (YP), gel strength, and thixotropy (Thixo) by The Bingham plastic rheological model to describe flow characteristics of the prepared mud fluid and mud fluid-modified graphene oxide, depending on two-parameter used in the drilling fluids industry, and can be described mathematically as follows:

$$\tau = \text{YP} + \text{PV} (\gamma)$$

where  $\tau$ ,  $\gamma$  donates shear stress and shear rate. From slope and intercept the values of

A parameter of the Bingham plastic rheological model PV is the slope of the shear stress-shear rate plot above the yield point.

Apparent viscosity (AV) is one-half of the dial reading ( $\text{AV} = 600 \text{ rpm reading} / 2$ ), plastic Viscosity PV is in centipoises (cP) calculated from the  $\text{PV} = 600 \text{ rpm reading} - 300 \text{ rpm reading}$ . Low values of PV imply that the mud has the ability to drill quickly due to the low viscosity of the drilling fluid produced from the drill bit, while higher values indicate an increase in the base viscosity and formation of colloidal fluid. Yield point (YP) assesses the ability to drill fluid to lift cuttings from the annulus. An increase in this value indicates that the drilling fluid

has the ability to lift and carry drilling cuttings better than other fluids of similar viscosity. The values (YP) can be obtained by subtracting the dial readings value at 300 rpm from PV's value. YP is the stress required to start moving the fluid and can be obtained by plotting the shear rate versus the shear stress, and it represents the intersection of the resulting straight line with the y-axis. Gel strength (GL,  $\text{lb}/100 \text{ ft}^2$ ) expresses the ability to drill fluid to suspend liquids in a constant state, and its value is identified at 3 rpm for 10 seconds and 10 minutes. Thixotropy is a time-dependent phenomenon, and its value depends on the time of share rate. Thixotropy was calculated by subtracting the reading of GL after 10 minutes from GL-10 sec.

#### 2.3.2.1. API Filter-Loss tests

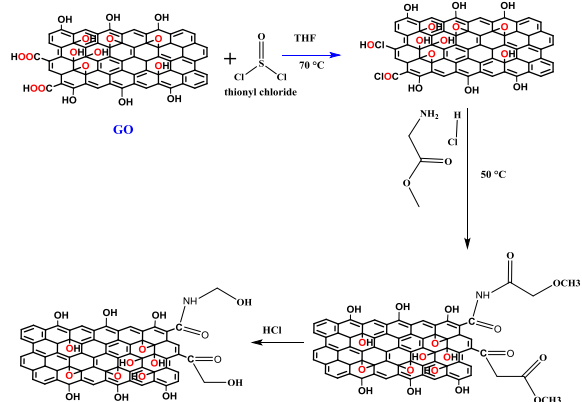
The API Fluid loss Test is known as mud filtrate's volume identifying after 30 minutes by API filter press (Fann, USA) at room temperature and pressure (100 psi).

### 3. Results and Discussion

This work depends on the synthesis of graphene oxide and the modification of its surface with a glycerin compound through the formation of a covalent bond between glycine and graphene oxide. To achieve this purpose, glycine was esterified with dry methanol alcohol in the presence of thionyl chloride and the formation of an ammonium chloride salt. The chlorination of graphene oxide was also done by thionyl chloride as well (**Scheme 1**). FTIR of glycine methyl ester hydrochloride is shown in **Figure 1a**.

**Figure 1a** shows the disappearance of the carboxyl group's peak (O-H stretching,  $3300 \text{ cm}^{-1}$ ), indicating the esterification process's success (Hassan et al., 2020). The strong-broad FTIR peaks at  $3000 \text{ cm}^{-1}$  is due to N-H stretching (amine salt). The C-H stretching of methylene appears at  $2840 \text{ cm}^{-1}$ , the strong peak at  $1752 \text{ cm}^{-1}$  is attributed to the carbonyl group in ester form. The peak at  $1695 \text{ cm}^{-1}$  indicates the formation of the amide group (primary amide). The peak at  $1465 \text{ cm}^{-1}$  is attributed to C-H bending (methylene group), while the peak at  $1450 \text{ cm}^{-1}$  is matched C-H bending of the methyl group. The peak at  $1125 \text{ cm}^{-1}$  referred to C-N stretching. The peak at  $1086$  is attributed to C-O stretching (ester). FTIR of GO and glycine-GO is shown in **Figure 1b**. GO showed a broad FTIR peak at  $3356 \text{ cm}^{-1}$  (O-H stretching) due to the presence of a large number of hydroxyl groups (Betiha, M. A. et al., 2020a). The peaks at  $1714 \text{ cm}^{-1}$  correspond to the carbonyl group in the carboxylic acid; the peaks at  $1069 \text{ cm}^{-1}$  indicate epoxy function groups' presence (Abdelrahman et al., 2018). By comparing the FTIR of graphene oxide with the glycine modified graphene oxide, it becomes clear that the peaks of the hydroxyl groups have slightly weakened and

broadened, indicating a part of the hydroxyl is consumed in the formation of the amide groups, and the broadness of the peak indicates the overlap between the hydroxyl and N-H groups.



**Scheme 1: Preparation of glycine methyl ester hydrochloride modified GO and glycine modified GO materials.**

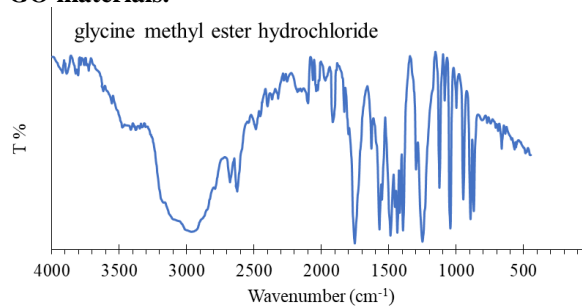


**Figure 1a: FTIR of glycine methyl ester hydrochloride salt**

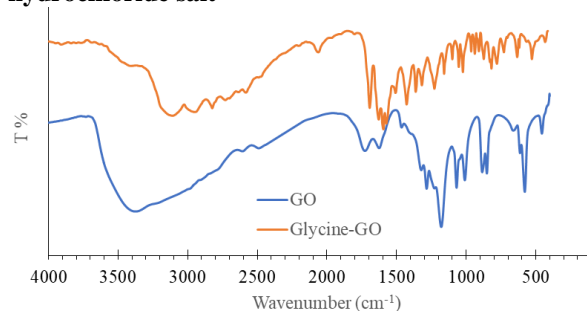


**Figure 1b: FTIR of GO and glycine modified-GO materials.**

Raman spectroscopy of bentonite and bentonite mixed with glycine-GO is shown in **Figure 2**. The bentonite's Raman spectrum shows three peaks before Raman shift of  $600\text{ cm}^{-1}$  ( $64, 249, 477\text{ cm}^{-1}$ ) corresponds to T–O–T substructure (breathing vibration mode) and is related to the  $\text{TO}_4$  size in the framework. The Raman peaks at  $616$  and  $913\text{ cm}^{-1}$  refer to the phyllosilicate vibration mode ( $\text{Si-O}_b\text{-Si}$ ) (Wang et al., 2015). It is clear the intensity of Raman bentonite peaks is affected by the addition of glycine-GO due to the change of phyllosilicate ratio in the overall sample, indicating the formation of glycine-

GO/bentonite nanocomposite. In addition, the D and G peaks of graphene oxide are easily seen at  $1357$  and  $1573\text{ cm}^{-1}$ .

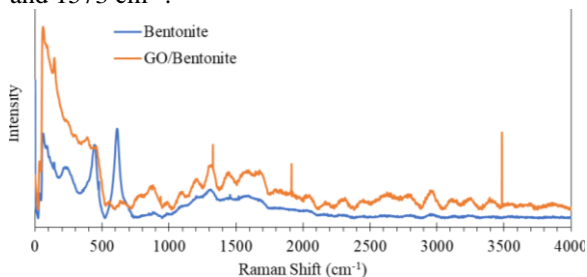


**Figure 2. Raman spectra of bentonite and glycine-GO/bentonite materials**

XRD of graphite, graphene oxide, and glycine modified graphene oxide is shown in **Figure 3a**. The XRD pattern shows steep peaks at  $26.51^\circ$  ( $0.34\text{ nm}$ ) and weak peaks at  $42.55^\circ$  (d-spacing of  $0.21\text{ nm}$ ),  $44.67^\circ$  (d-spacing of  $0.20\text{ nm}$ ), and  $54.67^\circ$  (d-spacing of  $0.17\text{ nm}$ ) (Al-Sabagh et al., 2016). In comparison with graphite, the sharp peak at  $26.51^\circ$  has diminished greatly with the emergence of a new peak at lower  $2\theta$  ( $10.62^\circ$ ), the obtained d-spacing is estimated to be two and a half times ( $0.83\text{ nm}$ ) as a result of the success of the oxidation process and the emergence of hydroxyl, epoxy and carboxyl groups, in addition to the water molecules associated with the outer surface of graphene oxide due to the presence of these functional groups, which has the ability to bond with water through hydrogen bonds. The distance between the layers of glycine-modified graphene oxide was increased, as the  $2\theta$  was shifted to a lower value ( $8.38^\circ$ ) to achieve the layer spacing of about  $1.05\text{ nm}$ , confirming the success of the interaction between glycine and graphene oxide.

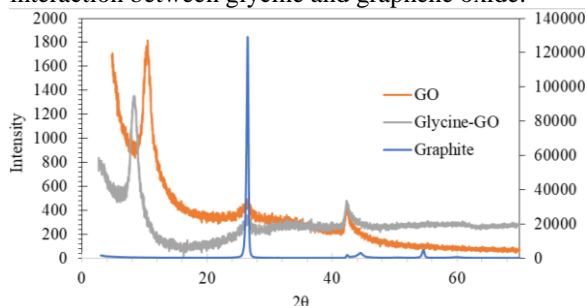


**Figure 3a: XRD of graphite, graphene oxide, and glycine modified graphene oxide**

**Figure 3b** shows the XRD of bentonite and glycine-GO/bentonite materials. The peaks of bentonite cleavage are evidently consistent with many peaks of montmorillonite, where the bentonite-XRD shows peaks at  $6.69^\circ$  ( $1.32\text{ nm}$ ),  $7.5^\circ$  ( $1.18\text{ nm}$ ),  $12.7^\circ$  ( $0.7\text{ nm}$ ),  $20.4^\circ$ ,  $21.38^\circ$  ( $0.42\text{ nm}$ ),  $25.37^\circ$  ( $0.35\text{ nm}$ ),  $27.15^\circ$  ( $0.33\text{ nm}$ ),  $29.5^\circ$  ( $0.3\text{ nm}$ ),  $34.35^\circ$  ( $0.26\text{ nm}$ ),  $35.27^\circ$  ( $0.25\text{ nm}$ ),  $36.86^\circ$  ( $0.24\text{ nm}$ ),  $37.07^\circ$  ( $0.24\text{ nm}$ ),  $40.5^\circ$  ( $0.22\text{ nm}$ ),  $42.94^\circ$  ( $0.21\text{ nm}$ ),  $45.19^\circ$  ( $0.2\text{ nm}$ ),  $45.97^\circ$  ( $0.2\text{ nm}$ ),  $47.9^\circ$  ( $0.19\text{ nm}$ ),  $50.66^\circ$  ( $0.18$

nm),  $55.64^\circ$  (0.17 nm),  $55.8^\circ$  (0.16 nm),  $60.44^\circ$  (0.15 nm),  $62.7^\circ$  (0.15 nm), and  $68.84^\circ$  (0.14 nm). After mixing glycine-modified graphene oxide, the peaks' intensities were reduced due to clay stack aggregation. The low  $2\theta$  peaks are shifted somewhat to a lower value due to the increase in the d-spacing between bentonite layers (Betiha, M. A. et al., 2020b).

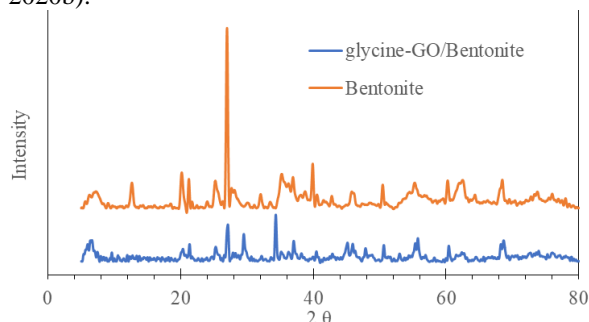


**Figure 3b: XRD of bentonite and glycine modified graphene oxide/bentonite materials.**

**Figure 4** shows an HRTEM image of graphene oxide, which has a great deal of transparency, confirming the oxidation process's success (Betiha, Mohamed A. et al., 2020). The slight opaque areas suggest some groupings of graphene oxide sheets.



**Figure 4: HRTEM of the glycine-graphene oxide material.**

### 3.2 Rheological properties of mud fluid

Shear rate/shear stress and rheology of the mud fluid presented in and **Figure 5**. It is clear that the drilling fluid sample shows shear-thinning behaviour against the increased shear rate. This behaviour can be attributed to the inability of the dispersed bentonite layers in the water due to the deterioration of the chemical bonds between the layers of the bentonite layers as the shear rate increased (Kazemi-Beydokhti and Hajiabadi, 2018). Moreover, increasing the shear rate forced the bentonite clay to flow along the direction of the shear rate, causing difficulty for bentonite aggregate to regenerate. The temperature has an obvious effect on the shear rate/shear stress curve, in which the shear stress decreases by

increasing the temperature from  $62^\circ\text{F}$  to  $100^\circ\text{F}$ , and then reducing significantly after  $200^\circ\text{F}$  and greatly affected at  $300^\circ\text{F}$  because the increase in temperature leads to a decrease in the water's viscosity, and thus reducing the viscosity of mud fluid.

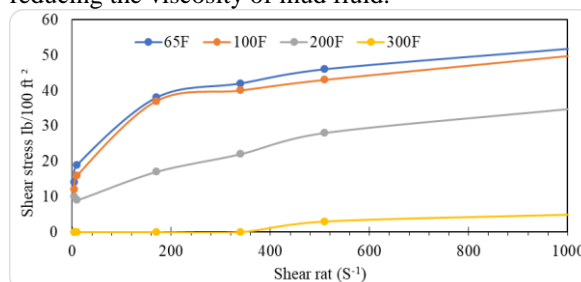


**Figure 5: The shear rate/shear stress of bentonite-based fluid at different temperatures**

**Figure 6** shows the rheological of bentonite-based mud at different temperatures. It is clear that all rheological parameters decrease as temperature increases from  $65^\circ\text{F}$  to  $300^\circ\text{F}$  except PV (**Figure 6**). The increase in PV value may be due to the swelling of bentonite in water increased by temperature. It should be noted here that the output ratio of the YP/PV can determine the shear-thinning behaviour of bentonite-based drilling fluids and others, as the increase in the value of the ratio result indicates an increase in the ability of the drilling fluid to suspend the drilling cuttings in the drilling fluid and thus gives better carrying capacity lift the cuts (Bourgoyne Jr et al., 1991; Srungavarapu et al., 2018). In our case, it was found that the ratio reduces dramatically as the ratio was 666.66, 514.28, 300, and 66.66 at temperatures of  $62^\circ\text{F}$ ,  $100^\circ\text{F}$ ,  $200^\circ\text{F}$ , respectively, and  $300^\circ\text{F}$ , which suggests the thermal instability of water-based bentonite at high temperatures.

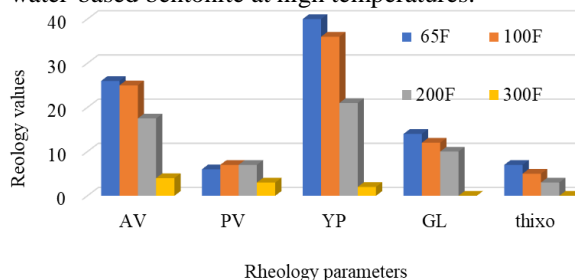


**Figure 6: Rheology of blank mud fluid different temperatures**

### 3.3. Rheological properties of glycine-GO/bentonite-based mud

**Figure 7** shows the shear rate/shear stress curve of glycine-GO/bentonite at a concentration glycine-GO of 2.66, 5.32, and 10.64% at a temperature of  $350^\circ\text{F}$ . The glycine-GO/bentonite-based mud shows shear thinning behaviour. The graph exhibits coincide the curves of the glycine-GO/bentonite concentration (2.66%, 5.32% and 10, 64%) with the blank mud fluid in the same trend, and the shear stress values increase as glycine-GO concentration increases from

2.66% to 5.32% and then declined at glycine-GO of 10.64%. The samples containing-glycine-GO show the shear stress values higher than bentonite-based water mud, indicating an interaction between glycine-GO and bentonite, causing an increase in mechanical friction between components of mud fluid (Kazemi-Beydokhti and Hajiabadi, 2018). All samples show shear-thinning behaviour due to the alignment of the glycine-GO nanolayers the fluidity of the flow (Kazemi-Beydokhti et al., 2018). Bearing in mind that the shear-thinning rheology is necessary and suitable for cutting bearing and pumping.

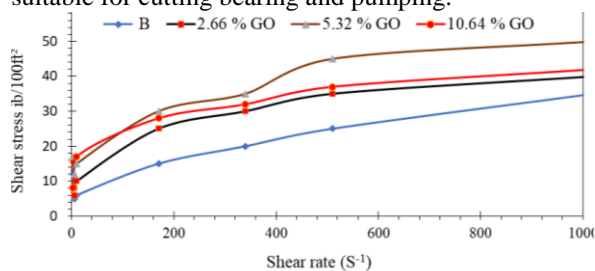


**Figure 7: The shear stress versus the shear rate of mud fluid at different concentrations**

The rheology of samples that included glycine-GO at a different concentration and temperature of 350 °F is presented in **Figure 8**.

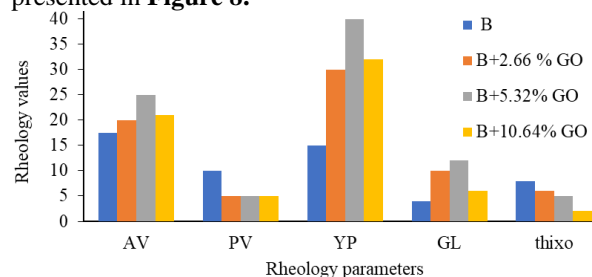


**Figure 8: Rheological properties of and glycine-GO/bentonite at different concentrations**

The addition of glycine-GO reduces the PV of fluids and increases the YP and gel strength. Shear rate against the viscosity of glycine-GO/bentonite is presented in **Figure 9**. The Graph reveals that the apparent viscosity of each concentration decreases greatly with increasing shear rate. This type of fluid displays a decreasing viscosity with an increasing shear rate known as non-Newtonian fluids (pseudoplastic).

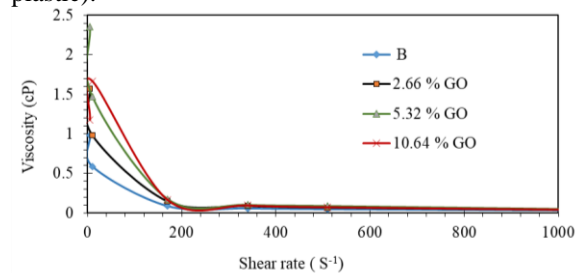


**Figure 9: The shear rate VS viscosity of bentonite and glycine-GO/bentonite at different concentrations**

Also, the increase in the temperature of the glycine-GO/bentonite resulted in a significant decrease in the apparent viscosity with an increase in shear rate, as shown in **Figure 10**. The curves graph shows the effect of temperature viscosity with increasing the shear rate at a concentration of 5.32%.

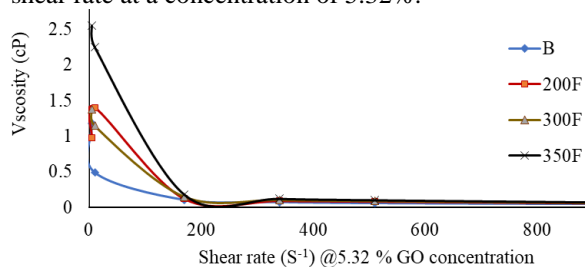


**Figure 10: Shear rate VS viscosity of glycine-GO/bentonite at different temperature and 5.32% GO.**

By comparing the viscosity between bentonite mud and glycine-GO/bentonite at different temperatures, a clear improvement is evident, and this improvement is attributed to the following reasons. Firstly, graphene oxide has a large surface area compared to bentonite clay, which led to an increase in the friction between the drilling fluid components and thus a clear improvement in viscosity. Secondly, graphene's possession of effective chemical groups has the ability to form hydrogen bond networks between graphene oxide surface's functional group (Medhekar et al., 2010) and water and bentonite layers, leading to increased bonding networks between the components of the drilling fluid (Inglefield Jr. et al., 2016). Third, the surface of graphene oxide is anionic, and thus the penetration of graphene oxide into the clay layers may be somewhat difficult, but the presence of the nitrogen atom increases the possibility of penetration of the graphene nanoscale layers into the bentonite layers, thus increasing the swelling of the bentonite will occur, increasing the occupied area of the liquid with bentonite, thus increasing the viscosity (Tunç and Duman, 2008). Finally, the increase in the added amount of graphene oxide shows an unclear increase and perhaps less compared to the lower ratio, as this behaviour is due to the increase of graphene oxide in solution, some plates may accumulate or aggregate on each other (Batiha, Mohamed A. et al., 2020), disrupting the chemical bonds of the buried layers from performing their function (creating hydrogen bonds), and thus the effect of this layer is null. Besides, the addition of 5.32% glycine-GO/bentonite shows the maximum shear stress, among others, maybe due to this amount matched the ratio of bentonite in the mud fluid, and

an increase in this ratio leads to more friction between glycine-GO layers.

The API filter loss of blank sample and glycine-GO/bentonite mud is presented in **Figure 11**. The blank sample's filter loss volume (bentonite-based mud) reaches up to 22 mL while the 2.66%-glycine-GO/bentonite mud runs 14.5 mL. However, as glycine-GO concentration increases to 5.32%, the filter loss has remarkably reduced to 12.6 mL due to glycine-GO's high performance as an additive-filter-loss-control. With the concentration increasing to 10.64 %, the volume re-increased to 16, 3 mL. Also, the mud cake thickness is presented in **Figure 12**.

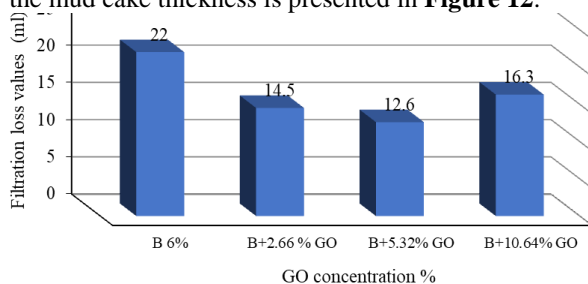


**Figure 11: Filtration loss of glycine-GO/bentonite at different concentrations.**

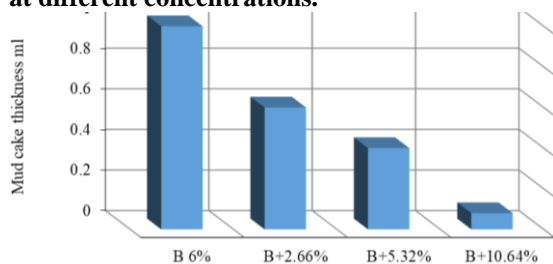


**Figure 12: Filtration loss of glycine-GO/bentonite at different concentration.**

#### 4. Conclusion

In this study, graphene oxide (GO) has been successfully synthesized from graphite, and its surface is modified by hydrolyzed glycine methyl ester hydrochloride. The chemical and physical properties are confirmed through FTIR, Raman, HRTEM, and XRD characterizations. An addition of glycine-GO/bentonite drilling fluid led to an increase in the performance of mud fluid, as indicated by better rheological properties. The addition of 2.66%-glycine-GO/bentonite resulted in a reduction in plastic viscosity from 15 to 10 cP and increased the yield point from 10 to 25 lbs/100 ft<sup>2</sup> and the GL increased from 6 to 13 lbs/100 ft<sup>2</sup>. The addition of 5.32%-glycine-GO/bentonite led to a reduction in plastic viscosity from 15 cp to 10 cp and an increase in yield point from 15 to 40 lbs/100 ft<sup>2</sup>, and the GL increased from 4 to 14 lbs/100 ft<sup>2</sup>. The significance of adding more than 5.32% glycine-GO/bentonite for enhancing rheological properties is not feasible. The filter loss reduced from 22 to 12.6 mm, and mud thickness reduced from 1 mL to 0.4 mm

#### References

- Abdelrahman, A.A., Betiha, M.A., Rabie, A.M., Ahmed, H.S., Elshahat, M.F., 2018. Removal of refractory Organo-sulfur compounds using an efficient and recyclable {Mo132} nanoball supported graphene oxide. *Journal of Molecular Liquids* 252, 121-132.
- Al-Sabagh, A.M., Betiha, M.A., Osman, D.I., Hashim, A.I., El-Sukkary, M.M., Mahmoud, T., 2016. Preparation and Evaluation of Poly(methyl methacrylate)-Graphene Oxide Nanohybrid Polymers as Pour Point Depressants and Flow Improvers for Waxy Crude Oil. *Energy & Fuels* 30(9), 7610-7621.
- Betiha, M.A., ElMetwally, A.E., Al-Sabagh, A.M., Mahmoud, T., 2020a. Catalytic Aquathermolysis for Altering the Rheology of Asphaltic Crude Oil Using Ionic Liquid Modified Magnetic MWCNT. *Energy & Fuels* 34(9), 11353-11364.
- Betiha, M.A., Mahmoud, T., Al-Sabagh, A.M., 2020b. Effects of 4-vinylbenzyl trioctylphosphonium- bentonite containing poly(octadecylacrylate-co-1-vinyldodecanoate) pour point depressants on the cold flow characteristics of waxy crude oil. *Fuel* 282, 118817.
- Betiha, M.A., Mohamed, G.G., Negm, N.A., Hussein, M.F., Ahmed, H.E., 2020. Fabrication of ionic liquid-cellulose-silica hydrogels with appropriate thermal stability and good salt tolerance as potential drilling fluid. *Arabian Journal of Chemistry* 13(7), 6201-6220.
- Bourgoyne Jr, A.T., Millheim, K.K., Chenevert, M.E., Young Jr, F.S., 1991. *Applied drilling engineering*.
- Faroughi, S.A., Pruvot, A.J.-C.J., McAndrew, J., 2018. The rheological behavior of energized fluids and foams with application to hydraulic fracturing: Review. *Journal of Petroleum Science and Engineering* 163, 243-263.
- Hassan, H.M.A., Betiha, M.A., El-Sharkawy, E.A., Elshaarawy, R.F.M., El-Assy, N.B., Essawy, A.A., Tolba, A.M., Rabie, A.M., 2020. Highly selective epoxidation of olefins using vanadium (IV) schiff base- amine-tagged graphene oxide composite. *Colloids and Surfaces A: Physicochemical and Engineering Aspects* 591, 124520.
- Inglefield Jr., D.L., Bodnar, R.J., Long, T.E., 2016. Hydrogen bond containing multiwalled carbon nanotubes in polyurethane composites. *Polymer Composites* 37(5), 1425-1434.
- Kazemi-Beydokhti, A., Hajiabadi, S.H., 2018. Rheological investigation of smart polymer/carbon nanotube complex on properties of water-based drilling fluids.

- Colloids and Surfaces A: Physicochemical and Engineering Aspects 556, 23-29.
- Kazemi-Beydokhti, A., Hajiabadi, S.H., Sanati, A., 2018. Surface Modification of Carbon Nanotubes as a Key Factor on Rheological Characteristics of Water-Based Drilling Muds. Iranian Journal of Chemistry and Chemical Engineering (IJCCE) 37(4), 1-14.
- Kelessidis, V.C., Christidis, G., Makri, P., Hadjistamou, V., Tsamantaki, C., Mihalakis, A., Papanicolaou, C., Foscolos, A., 2007. Gelation of water–bentonite suspensions at high temperatures and rheological control with lignite addition. Applied Clay Science 36(4), 221-231.
- Kelessidis, V.C., Maglione, R., Tsamantaki, C., Aspirotakis, Y., 2006. Optimal determination of rheological parameters for Herschel–Bulkley drilling fluids and impact on pressure drop, velocity profiles and penetration rates during drilling. Journal of Petroleum Science and Engineering 53(3), 203-224.
- Kosynkin, D.V., Ceriotti, G., Wilson, K.C., Lomeda, J.R., Scorsone, J.T., Patel, A.D., Friedheim, J.E., Tour, J.M., 2012. Graphene oxide as a high-performance fluid-loss-control additive in water-based drilling fluids. ACS applied materials & interfaces 4(1), 222-227.
- Li, M.-C., Wu, Q., Song, K., De Hoop, C.F., Lee, S., Qing, Y., Wu, Y., 2016. Cellulose nanocrystals and polyanionic cellulose as additives in bentonite water-based drilling fluids: rheological modeling and filtration mechanisms. Industrial & Engineering Chemistry Research 55(1), 133-143.
- Luo, Z., Wang, L., Pei, J., Yu, P., Xia, B., 2018. A novel star-shaped copolymer as a rheology modifier in water-based drilling fluids. Journal of Petroleum Science and Engineering 168, 98-106.
- Marcano, D.C., Kosynkin, D.V., Berlin, J.M., Sinitskii, A., Sun, Z., Slesarev, A., Alemany, L.B., Lu, W., Tour, J.M., 2010. Improved Synthesis of Graphene Oxide. ACS Nano 4 (8) .4814-4806
- Medhekar, N.V., Ramasubramaniam, A., Ruoff, R.S., Shenoy, V.B., 2010. Hydrogen Bond Networks in Graphene Oxide Composite Paper: Structure and Mechanical Properties. ACS Nano 4(4), 2300-2306.
- Ponmani, S., Nagarajan, R., Sangwai, J.S., 2016 . Effect of nanofluids of CuO and ZnO in polyethylene glycol and polyvinylpyrrolidone on the thermal, electrical, and filtration-loss properties of water-based drilling fluids. SPE Journal 21(02), 405-415.
- Pytlakowska, K., Kozik, V., Matussek, M., Pilch, M., Hachuła, B., Kocot, K., 2016. Glycine modified graphene oxide as a novel sorbent for preconcentration of chromium, copper, and zinc ions from water samples prior to energy dispersive X-ray fluorescence spectrometric determination. RSC Advances 6(49), 4-2836 .42844
- Rafati, R., Smith, S.R., Haddad, A.S., Novara, R., Hamidi, H., 2018. Effect of nanoparticles on the modifications of drilling fluids properties: A review of recent advances. Journal of Petroleum Science and Engineering 161, 61-76.
- Saleh, T.A., Rana, A., Arfaj, M.K., 2020. Graphene grafted with polyethyleneimine for enhanced shale inhibition in the water-based drilling fluid. Environmental Nanotechnology, Monitoring & Management 14, 100348.
- Srungavarapu, M., Patidar, K.K., Pathak, A.K., Mandal, A., 2018. Performance studies of water-based drilling fluid for drilling through hydrate bearing sediments. Applied Clay Science 152, 211-220.
- Tunç, S., Duman, O., 2008. The effect of different molecular weight of poly(ethylene glycol) on the electrokinetic and rheological properties of Na-bentonite suspensions. Colloids and Surfaces A: Physicochemical and Engineering Aspects 317(1), 93-99.
- Vryzas, Z., Mahmoud, O., Nasr-El-Din, H.A., Kelessidis, V.C., 2015. Development and testing of novel drilling fluids using Fe<sub>2</sub>O<sub>3</sub> and SiO<sub>2</sub> nanoparticles for enhanced drilling operations, International petroleum technology conference. International Petroleum Technology Conference.
- Wang, A., Freeman, J.J., Joliff, B.L., 2015. Understanding the Raman spectral features of phyllosilicates. Journal of Raman Spectroscopy 46(10), 829-845.
- Xuan, Y., Jiang, G., Li, Y., 2014. Nanographite Oxide as Ultrastrong Fluid-Loss-Control Additive in Water-Based Drilling Fluids. Journal of Dispersion Science and Technology 35(10), 1386.1392-
- Zhong, H., Qiu, Z., Huang, W., Sun, D., Zhang, D., Cao, J., 2015. Synergistic stabilization of shale by a mixture of polyamidoamine dendrimers modified bentonite with various generations in water-based drilling fluid. Applied Clay Science 114, 359..369-